

AperTO - Archivio Istituzionale Open Access dell'Università di Torino

The Cardiac Caval Index: Improving Noninvasive Assessment of Cardiac Preload

This is the author's manuscript

Original Citation:

Availability:

This version is available <http://hdl.handle.net/2318/1829533> since 2022-02-16T12:55:43Z

Published version:

DOI:10.1002/jum.15909

Terms of use:

Open Access

Anyone can freely access the full text of works made available as "Open Access". Works made available under a Creative Commons license can be used according to the terms and conditions of said license. Use of all other works requires consent of the right holder (author or publisher) if not exempted from copyright protection by the applicable law.

(Article begins on next page)

The cardiac caval index. Improving non-invasive assessment of cardiac preload

**Dr. Leonardo Ermini¹, Dr. Stefano Seddone¹, Dr. Piero Policastro², Prof. Luca Mesin²,
Dr. Paolo Pasquero³, Prof. Silvestro Roatta¹**

¹Laboratory of Integrative Physiology, Department of Neuroscience, Università di Torino, c.so Raffaello 30, 10125, Torino, Italy

²Mathematical Biology and Physiology, Department of Electronics and Telecommunications, Politecnico di Torino, c.so Duca degli Abruzzi 24, 10129, Torino, Italy

³Department of Medical Sciences, Università di Torino, c.so Achille Mario Dogliotti 14, 10126 Torino, Italy

ORCID:

LE: 0000-0002-3362-0623
SS: 0000-0002-1909-871X
PPo: 0000-0002-3154-7426
LM: 0000-0002-8239-2348
PPa: 0000-0002-5802-3446
SR: 0000-0001-7370-2271

Running title

The Cardiac Caval Index

Corresponding author: Leonardo Ermini, c.so Raffaello 30, 10125, Torino, Italy.

E-mail: leonardo.ermi@unito.it. Phone: +39 011 6708164.

36 **Abstract**

37 Inferior Vena Cava (IVC) pulsatility quantified by the Caval Index (CI) is characterized by
38 poor reliability, also due to the irregular magnitude of spontaneous respiratory activity
39 generating the major pulsatile component. The aim of this study was to test whether the IVC
40 cardiac oscillatory component could provide a more stable index (Cardiac CI - CCI) compared
41 to CI or respiratory CI (RCI). Nine healthy volunteers underwent long-term monitoring in
42 supine position of IVC, followed by 3 min Passive Leg Raising (PLR). CI, RCI and CCI were
43 extracted from video recordings by automated edge-tracking and CCI was averaged over each
44 respiratory cycle (aCCI). Cardiac Output (CO), Mean Arterial Pressure (MAP) and Heart Rate
45 (HR) were also recorded during baseline (1 min prior to PLR) and PLR (first minute). In
46 response to PLR, all IVC indices decreased ($p < 0.01$), CO increased by $4 \pm 4\%$ ($p = 0.055$) while
47 HR and MAP did not vary. The Coefficient of Variation (CoV) of aCCI ($13 \pm 5\%$) was lower
48 than that of CI ($17 \pm 5\%$, $p < 0.01$), RCI ($26 \pm 7\%$, $p < 0.001$) and CCI ($25 \pm 7\%$, $p < 0.001$). The
49 mutual correlations in time of the indices were 0.81 (CI-RCI), 0.49 (CI-aCCI) and 0.2 (RCI-
50 aCCI). Long-term IVC monitoring by automated edge-tracking allowed us to evidence that 1)
51 respiratory and averaged cardiac pulsatility components are uncorrelated and thus carry
52 different information and 2) the new index aCCI, exhibiting the lowest CoV while maintaining
53 good sensitivity to blood volume changes, may overcome the poor reliability of CI and RCI.

54
55 **Key Words:** inferior vena cava; passive leg raising; volume status; fluid responsiveness;
56 automatic edge tracking.

57

58 Introduction

59 In the clinical setting, deciding whether and what amount of fluid to administer
60 intravenously to a patient, i.e., the prediction of fluid responsiveness, is a long-standing open
61 issue, whose relevance is paramount. Indeed, it has been shown that only half of the
62 haemodynamic unstable patients exhibits a positive outcome after a fluid challenge¹, while the
63 remaining ones are exposed to the risk of fluid overload²⁻⁴. Since no satisfactory solution to
64 this problem has been found yet, improvements in the existing techniques as well as new
65 methodological approaches are constantly investigated⁵⁻⁹.

66 Due to its fast and non-invasive approach, the echographic assessment of the Inferior Vena
67 Cava (IVC) pulsatility is a widely adopted monitoring technique⁷. From the analysis of
68 pulsatility, it is possible to infer about the mechanical characteristics of blood vessels, such as
69 stiffness and compliance, and about their determinants, such as blood pressure, blood volume,
70 vessel tone, etc. (Mesin et al., *submitted*). IVC pulsatility is often quantified by means of the
71 Caval Index (CI), which conveniently normalizes the respirophasic diameter variation ($d_{\max} -$
72 d_{\min}) to d_{\max} , thus accounting for individual differences in IVC size (d_{\max} and d_{\min} being the
73 maximum and minimum diameters, as measured at the end of the expiratory and inspiratory
74 phases, respectively). However, this index suffers of a large variability and, consequently, of
75 poor reliability¹⁰⁻¹². Based on the development of new image processing algorithms, several
76 sources of variability were recently investigated and compensated for, e.g., by tracking the
77 displacement of the vessel with respect to the ultrasound (US) probe^{13,14} and by averaging the
78 measurements over several IVC diameters in either short¹⁵ or long axis^{14,16}, which contributed
79 to improve the repeatability of the measurements^{15,16}. However, a major source of variability
80 in the respirophasic oscillation of IVC size is the intrinsic variability of spontaneous respiratory
81 activity, in terms of magnitude, frequency and relative extent of thoracic/diaphragmatic
82 respiration^{17,18}, all these aspects providing consistent effects on IVC pulsatility¹⁸⁻²¹. A possible
83 solution to this problem was originally suggested by Nakamura²² who proposed to consider
84 the cardiac component of IVC pulsatility rather than the respiratory. The issue was followed-
85 up in few subsequent studies^{15,16,19,23}. In these studies, the automated analysis of US video
86 clips yielded the continuous description of IVC size changes with high time resolution (equal
87 to the frame rate of the US video recording), so that the cardiac and respiratory components of
88 IVC pulsatility could be easily separated, based on their different frequency contents, and
89 independently analysed^{15,16,23}. On this basis, the respiratory CI (RCI) and the cardiac CI (CCI),
90 specifically quantifying the respiratory and cardiac component of IVC pulsatility, were
91 introduced and compared. The results showed that also the CCI could be used as an index of
92 vascular filling^{22,23} and that it was characterized by a lower variability (as quantified by the
93 coefficient of variation, CoV) than the RCI, although, contrary to the expectation, not lower
94 than the variability of the CI¹⁶. Two reasons may possibly explain this observation: 1) the
95 above mentioned results refer to index variability over different subjects and measurement
96 sessions, while the actual CCI variability over time has never been assessed; 2) the cardiac
97 pulsatility may still be affected by a respiratory modulation, as apparent from published
98 recordings^{16,24} and confirmed in preliminary observations. However, to our knowledge, all
99 studies generally considered only short time intervals lasting 10-15 s, and the time correlation
100 between pulsatile components has never been investigated.

101 We hypothesized that 1) by further improving the signal processing we could effectively
102 reduce the respiratory modulation of CCI and obtain a more stable hemodynamic index of
103 vascular filling; 2) due to its different nature, the CCI could differ from RCI and CI in terms of
104 time course and responsiveness to fluid challenges.

105 To this purpose, continuous and long-duration recordings of B-mode IVC imaging were
 106 performed with the help of a dedicated probe holder, in resting conditions and during a
 107 simulated fluid challenge, as produced by passive leg raising (PLR).

108 **Materials and Methods**

109 *Subjects*

110 Nine healthy volunteers (7 M, 2 F, age 34 ± 9) were included in the study, with the only
 111 exclusion criteria being a poor quality of the echographic imaging. The study was approved by
 112 the Ethics Committee of the University of Torino (March 23, 2015) and all participants gave
 113 their informed consent according to the principles of the Helsinki Declaration.

114 *Experimental set-up and protocol*

115 Participants remained supine on a clinical bed for at least 30 min before starting the
 116 experiment, in order to stabilize the equilibrium between fluid compartments^{19,25}. A two-
 117 dimensional B-mode longitudinal view of the IVC was recorded by means of a MyLab 25 Gold
 118 system (ESAOTE, Genova, Italy) equipped with a convex 2-5 MHz US probe, according to a
 119 *sub-xyphoid* transabdominal long axis approach (2-3cm caudal to the right atrial junction)²⁶.
 120 To achieve long-lasting ultrasound (US) monitoring, we made use of a probe holder, as
 121 successfully implemented in previous studies for stable echo-Doppler monitoring of arteries
 122 and veins of upper and lower limbs^{9,27-30}. In the present case, the probe holder was stemming
 123 from one side of the bed and its 40-cm long horizontal arm was allowed to freely rotate about
 124 a joint at one of its ends. The US probe, located at the other end, due to its own weight, could
 125 then exert a light pressure on the abdomen and maintain adequate acoustic contact,
 126 accommodating with virtually vertical displacements the small abdominal movements during
 127 respiration. This arrangement allowed us to continuously monitor the IVC for the whole
 128 duration of the protocol (4 min).
 129

Variable	Baseline	PLR	DELTA %	p-value
Heart Rate (bpm)	59 ± 9	59 ± 10	0 ± 3	0.82
Mean Arterial Pressure (mmHg)	89 ± 11	90 ± 9	1 ± 6	0.43
Cardiac Output (L/min)	5.0 ± 0.8	5.1 ± 0.7	4 ± 4	0.03
Caval Index (%)	27 ± 6	19 ± 7	-31 ± 17	0.004
Respiratory Caval Index (%)	14 ± 4	9 ± 4	-35 ± 17	0.004
averaged Cardiac Caval Index (%)	13 ± 4	9 ± 4	-28 ± 21	0.008

130 **Table 1.** Averaged values of Heart Rate, Mean Arterial Pressure, Cardiac Output, Caval Index, Respiratory Caval
 131 Index, and averaged Cardiac Caval Index in absolute values, during baseline and PLR, and in terms of percentage
 132 variation during PLR w.r.t the mean baseline value (DELTA). Values are expressed as MEAN \pm STD. Last
 133 column reports the p-value of the paired statistical comparison, by means of a paired Wilcoxon signed rank test,
 134 among the two distributions of PLR and baseline individually averaged values.

135

136
137
138
139
140
141
142
143
144
145
146
147
148

The experimental protocol consisted of 1 min of rest in supine position (baseline), followed by 3 min during which the legs were passively raised and maintained at about 45 deg (passive leg raising, PLR) and 1 min of rest, again in supine position. During the entire protocol, the US video of the IVC longitudinal section (in the sagittal plane) was recorded for the subsequent processing and analysis. In addition, Heart Rate (HR), Mean Arterial Pressure (MAP) and Cardiac Output (CO) were non-invasively monitored by photoplethysmography (CNAP®, CNSystems Medizintechnik, Graz, Austria) while breathing was monitored by means of a custom-made strain gauge band placed around the chest (the recorded signal is referred to as Breath in the following). All these signals were digitally and synchronously recorded by a general-purpose acquisition board (Micro 1401 IImk, CED, Cambridge, UK, with Spike2 software): IVC videos were acquired at about 30 fps while HR, MAP, CO and breathing were sampled at 10 Hz.

149 *IVC segmentation*

150 US videos were processed by a custom-made software (implemented in MATLAB 2020a,
151 The MathWorks, Natick, MA) for IVC edge-tracking. The routines were based on a previously
152 developed algorithm¹⁴. The tracking algorithm was improved to attenuate the effect of small
153 drifts, which would produce detrimental effects with videos of long duration considered here
154 (manuscript in preparation). The edges of the IVC were estimated as previously described¹⁴,
155 by sampling along 21 directions crossing the blood vessel, considering a portion selected by an
156 operator (PPo), who was blinded to the results. Along each direction, the software estimated
157 the US pixel intensity by interpolation. Then, abrupt variations of this estimated US intensity
158 were identified as the locations of the two IVC edges along the considered direction (see Mesin
159 et al.¹⁴ for additional details). The length of the segment between each couple of points placed
160 on the upper and lower vein edges was the IVC diameter along that direction.

161 The median axis of the vein was estimated (as the mean of the two sampled edges),
162 interpolated by a second order polynomial and used to rotate the 21 diameters mentioned above
163 to be orthogonal to it. By considering all frames of the US video, each diameter was a time
164 series. High frequency contributions in these time series of diameters (mostly related to
165 superimposed noise) were removed. For the identification of the cut-off frequency, the power
166 spectrum density (PSD) of the diameters was first computed (Burg method, with order 40³¹),
167 from which the highest frequency of our interest was identified as follows. First, we have
168 searched for a peak in the PSD between 40bpm and 120bpm, which reflected the cardiac
169 component. Then, the median (across diameters) of peak frequencies (mf) was computed (this
170 parameter was used later to define the cut-off frequency of the filter). Then, a portion of 15 mm
171 around the position of the diameter showing the highest peak of the cardiac component was
172 selected (assuming that such a diameter provided reliable information on the cardiac
173 contribution and that it was less affected by noise than the other diameters). Upper and lower
174 border points of this portion of the vein were then interpolated with two straight lines. Finally,
175 the *mean IVC diameter*, for each frame, was calculated as the area of the IVC section
176 considered above, divided by its length (i.e., 15 mm).

177 Such a mean diameter was low pass filtered, with cut-off frequency equal to $mf + 0.5Hz$
178 (Chebyshev of type I, stop band starting at $mf + 1.5Hz$, minimum attenuation of 30 dB,
179 passband from 0 to $mf + 0.5Hz$ with ripple of 0.5 dB) and indicated with *dIVC*.

180 The respiratory and cardiac components of IVC pulsatility were estimated from the mean
181 diameter just obtained. The respiratory diameter, indicated as *R-dIVC*, was estimated by the
182 first step of the Empirical Mode Decomposition applied to the mean diameter. Specifically,
183 two curves were first obtained by interpolating the local maxima and the local minima of *dIVC*.

184 The curve *R-IVC* was defined as the mean of these two curves. Notice that this technique allows
185 to estimate each respiration cycle. On the other hand, a filter with fixed passband was used in
186 previous works ¹⁶: such a filter had lower performances than the one used here, especially with
187 our long recordings, in which respiration cycles could have very different durations (thus, being
188 attenuated differently by a fixed filter). The cardiac diameter, called *C-dIVC*, was computed as
189 $C-dIVC = dIVC - R-dIVC + s-dIVC$ and is equivalent to the mean diameter deprived of the
190 respiratory oscillations. The term *s-dIVC* indicates the lowpass filtered mean diameter with cut-
191 off 0.05 Hz (Chebyshev filter of type I, stop band starting at 0.5 Hz, minimum attenuation of
192 30 dB, passband ripple of 0.5 dB), where only the *slow* sub respiratory frequencies are left.
193 This low pass filter was chosen in order to remove any oscillation and keep only the low
194 frequency trend reflecting slow IVC size variations induced by the PLR.

195 At this point of the analysis, the three diameters, *dIVC*, *R-dIVC* and *C-dIVC* were available
196 as time series (see Fig. 1) and were used to estimate the collapsibility indicators Caval Index
197 (CI), Respiratory Caval Index (RCI) and Cardiac Caval Index (CCI) respectively, according to
198 the usual formula: $(d_{\max} - d_{\min})/d_{\max}$ (Fig. 1, bottom). Note that, while for CI and RCI one
199 estimate per respiratory cycle is obtained, the CCI yields one estimate per cardiac cycle.

200 In addition, an *averaged* version of the CCI, aCCI, was computed by averaging the CCI
201 over distinct respiratory cycles. The aCCI estimates could then be considered synchronous with
202 CI and RCI (one estimate per respiratory cycle).

203 *Data analysis*

204 HR, MAP and CO were exported from Spike2 software to MATLAB® (version 2020b) for
205 off-line analysis. As a first step, they were aligned in time with the time-series of the IVC
206 collapsibility indexes, computed separately as explained above, that presented a non-uniform
207 sampling rate due to their nature. Indeed, CI, RCI and aCCI had one sample per respiratory
208 cycle while CCI one per heartbeat: the sample location in time, within the respiratory cycle,
209 was arbitrary and we chose to be at the minimum of the IVC diameter component for all the
210 three indexes.

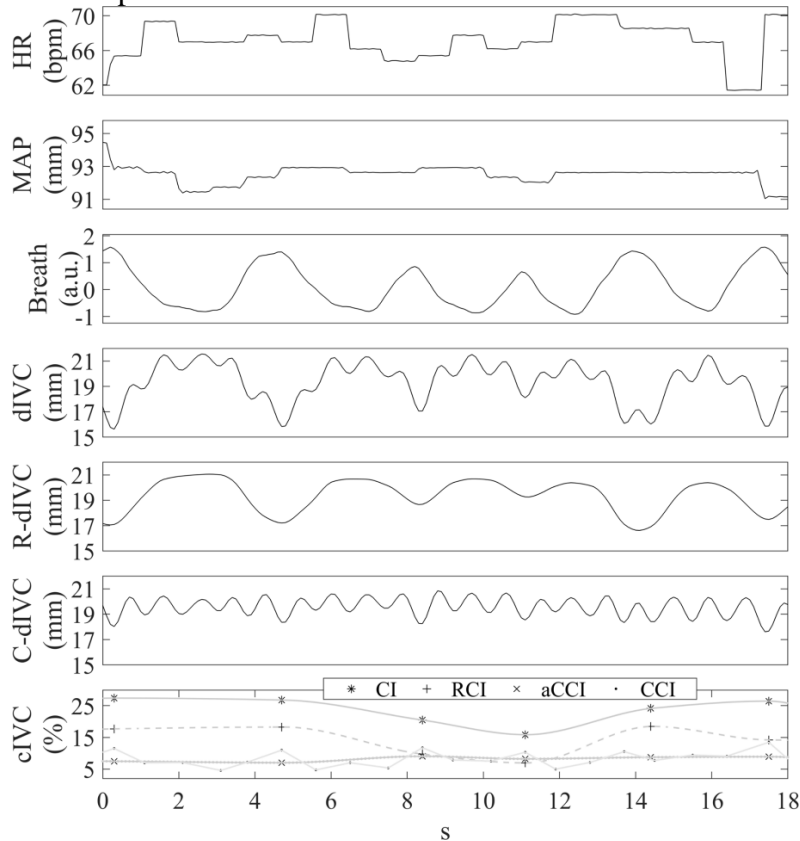
211 The intra-subject variability in time of each IVC collapsibility index was quantified during
212 baseline by the coefficient of variation ($CoV = (STD / MEAN) \times 100$) and averaged across all
213 subjects. The correlation of time course in baseline was tested among CI, RCI and aCCI, for
214 each subject, using the Pearson correlation coefficient (ρ); then, the mean ρ across subjects was
215 computed by averaging the individual ρ values after a Fisher Z-transformation and
216 subsequently applying an inverse transformation to the result.

217 In order to perform the correlation of IVC indices with other signals, they were resampled
218 at 10 Hz, after a shape-preserving piecewise cubic interpolation. This was necessary to test the
219 correlation of CCI and aCCI with the respiratory pattern. However, since the delay between
220 the respiratory effort and the resulting changes in size of the IVC cannot be assumed constant
221 neither across subject nor over time, the normalized cross-correlation function on the
222 appropriately standardized signals, instead of Pearson correlation coefficient, was employed
223 and its maximum value, irrespective of the delay, was chosen as the correlation coefficient (ρ).
224 Then, the ρ values obtained were averaged across subjects using the Fisher transformation as
225 explained above.

226 The response to the PLR is known to take place within the first minute after raising the legs
227 ³² and, for each of the variables, it was assessed as the difference between the mean value
228 calculated during the first minute of PLR and during the whole baseline (1 min), as $DELTA =$
229 $PLR - baseline$, and considered in both absolute and relative (percentage) terms. For both basal
230 and DELTA values, mutual correlations among CI, RCI and aCCI were quantified by the
231 Pearson correlation coefficient, presented along with the 95% confidence interval in between

232 brackets. The effect of PLR on each variable was assessed considering the distribution of
 233 DELTA values and testing if the mean differed from zero with a level of significance set at
 234 0.05, by means of the Wilcoxon signed rank test. The same test was used to compare the
 235 variability in time (as expressed by the CoV) of aCCI with CI and RCI. The IVC indices
 236 accuracy in predicting the subject response to the simulated fluid challenge, as induced by PLR,
 237 was analysed by means of Receiver Operating Characteristic (ROC) curves built using a 10%
 238 increase in CO as marker of fluid responsiveness^{6,33}.

239 Finally, it is worth to mention that, given the non-uniform sampling rate for the IVC
 240 collapsibility indexes, their average time course, across subjects, was obtained by averaging
 241 the interpolated curves.



242
 243 **Fig. 1.** Tracings from a representative subject, in resting condition. The time course of each one of the following
 244 variables is shown: Heart Rate (HR), Mean Arterial Pressure (MAP), Respiration (Breath), Inferior Vena Cava
 245 (IVC) respiratory (R-dIVC) and cardiac (C-dIVC) components of the native diameter trace (dIVC) and their
 246 respective indexes, namely Caval Index (CI), Respiratory Caval Index (RCI) and averaged Cardiac Caval Index
 247 (aCCI). In the latter graph, the markers indicate the exact sample of each IVC collapsibility indexes, as described
 248 in the legend, while the continuous grey lines are the respective cubic interpolation that were superimposed for a
 249 better visualization.

250 Results

251 Basal conditions

252 An example of the original tracings from a representative subject is shown in Figure 1
 253 which includes the continuous recordings of some systemic variables like HR, MAP, and
 254 respiratory activity as well as variables extracted from the US monitoring of the IVC, i.e., the
 255 IVC diameter (average diameter of the considered IVC segment), the respiratory diameter (high
 256 frequency components are filtered out) and the cardiac diameter (the respiratory component is

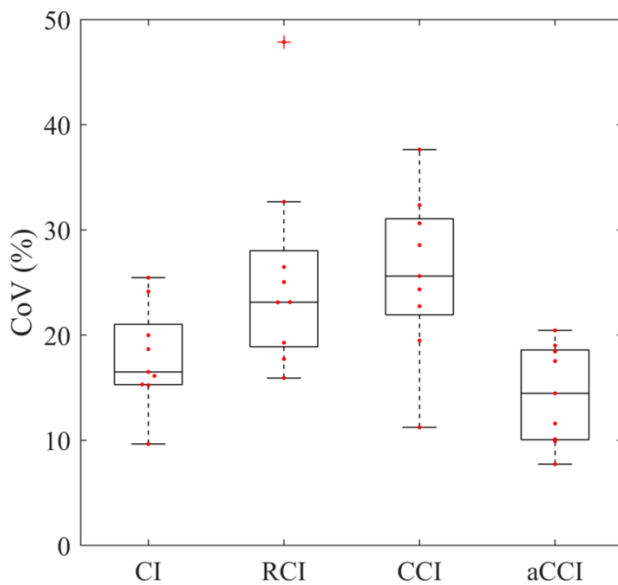
257 filtered out). At the bottom of the figure are the different indices, automatically calculated. Two
258 aspects need to be observed.

259 1) A strong correspondence exists between the magnitude of respiratory acts and the
260 respiratory changes in IVC diameter. Accordingly, CI and RCI (bottom) are also
261 modulated by the depth of respiration, in particular, it is worth to notice how CI and
262 RCI drop (the variation is in the order of 10%) around the fourth second of the
263 recording, concomitantly with a reduced inspiratory depth, as revealed by the Breath
264 signal.

265 2) Even the cardiac pulsatility is modulated by the respiratory activity. Accordingly, such
266 modulation is preserved in CCI and affects its variability in time.

267 We first tested whether the averaging over single respiratory cycles, as implemented for
268 the calculation of aCCI, was effective in reducing the respiratory modulation affecting CCI:
269 the averaged maxima of cross-correlation with respiration dropped from 0.4 (CCI) to 0.02
270 (aCCI).

271



272

273 **Fig. 2.** Coefficient of Variation (CoV) of collapsibility indexes of the inferior vena cava. The CoV distributions
274 across subjects computed during baseline are shown for Caval Index (CI), Respiratory Caval Index (RCI), Cardiac
275 Caval Index (CCI) and averaged Cardiac Caval Index (aCCI). The red dots indicate the individual data.

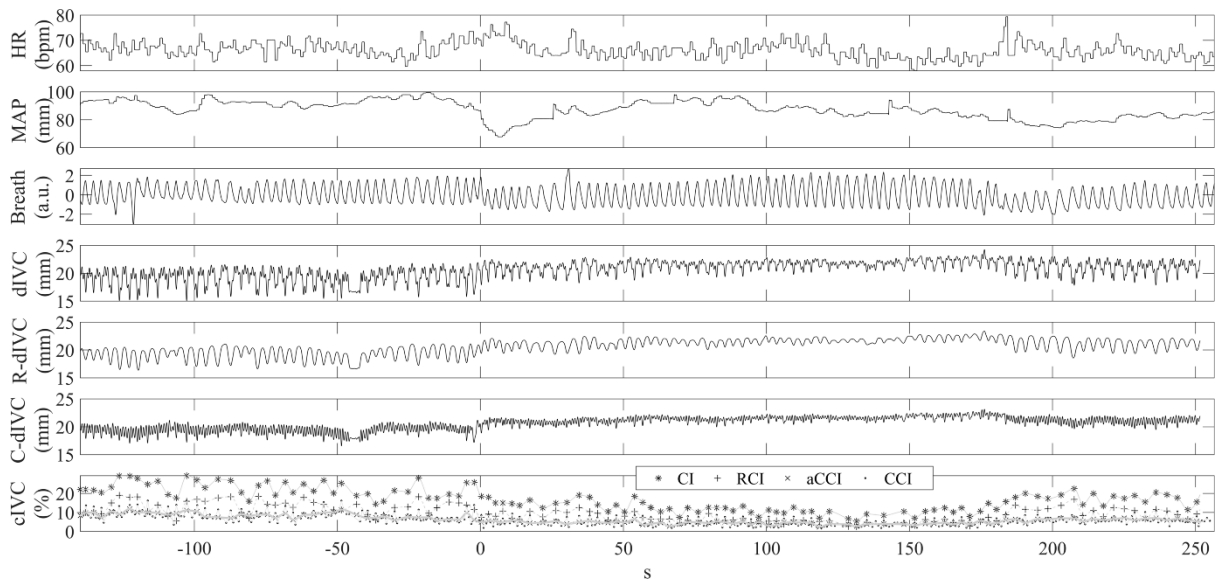
276

277 Then, we tested whether this new feature was effective in reducing the overall variability
278 in time, as assessed by the CoV. In Figure 2 it is possible to observe the distribution of the
279 individual CoVs, depicted by means of box and whiskers plots, for each IVC collapsibility
280 index, including the original CCI. The MEAN \pm STD CoV values of CI, RCI, CCI and aCCI
281 are, respectively, 17 ± 5 %, 26 ± 7 %, 25 ± 7 %, 13 ± 5 %. As expected, aCCI exhibited a lower
282 variability than CCI. The improved stability over time can also be observed by comparing the
283 corresponding tracings in Figure 1. Moreover, aCCI also achieved a lower CoV than CI
284 ($p < 0.01$).

285 *Response to PLR*

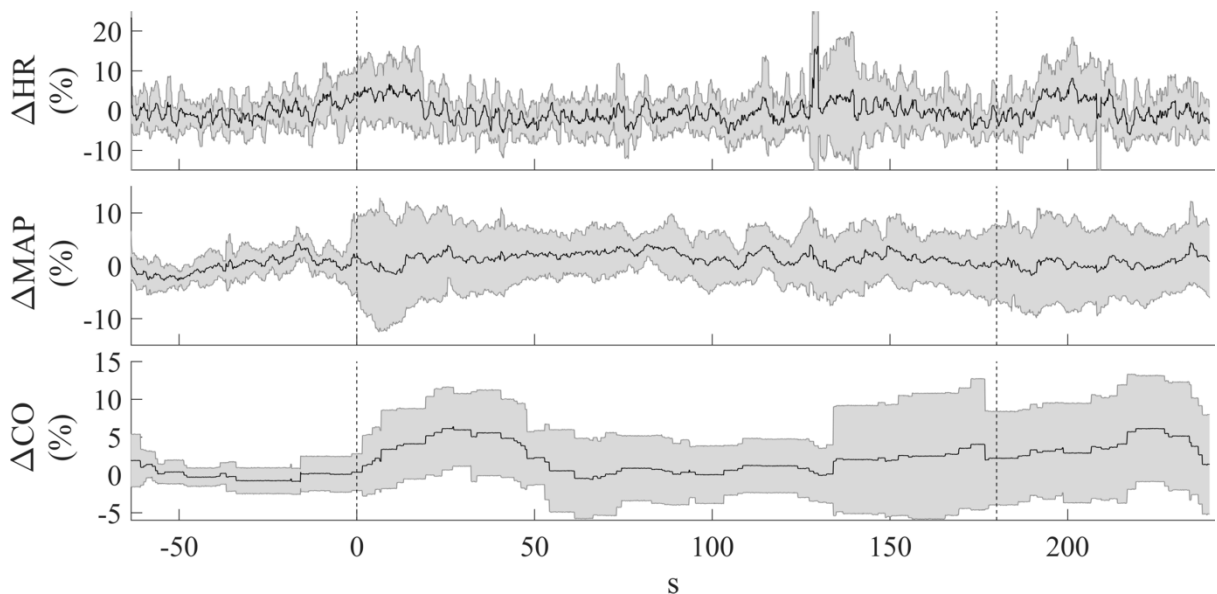
286 On a different timescale, the full representation of the response to PLR of a representative
287 subject is shown in Figure 3. It can be observed that during PLR, starting at time 0 s, both
288 cardiac and respiratory pulsatile components are reduced, and that the IVC diameter is
289 increased. This results in a reduction of all indices during PLR, as displayed at the bottom.

290



291
 292 **Fig. 3.** Example of a complete individual recording. The time course of each one of the following variables is
 293 shown: Heart Rate (HR), Mean Arterial Pressure (MAP), Respiration (Breath), Inferior Vena Cava (IVC)
 294 respiratory (R-dIVC) and cardiac (C-dIVC) components of the native diameter trace (dIVC) and their respective
 295 indexes, namely Caval Index (CI), Respiratory Caval Index (RCI) and averaged Cardiac Caval Index (aCCI). In
 296 the latter graph, the markers indicate the exact sample of each IVC collapsibility indexes, as described in the
 297 legend, while the continuous grey lines are the respective cubic interpolation that were superimposed for a better
 298 visualization.
 299

300 In Figure 4, the averaged (across subjects) time course of HR, MAP and CO are presented
 301 in terms of percentage changes with respect to the mean baseline value (i.e., DELTA in
 302 percentage terms). It can be observed that at the beginning of PLR (time 0 s), HR and MAP
 303 exhibit only small fluctuations while CO immediately begins to rise reaching a peak at around
 304 30 s and returning to the basal value at around 60 s, before the end of PLR (180 s).
 305



306
 307 **Fig. 4.** Haemodynamic variables averaged (across subjects) time course. Percentage changes with respect to the
 308 mean baseline value of Heart Rate (Δ HR), Mean Arterial Pressure (Δ MAP) and Cardiac Output (Δ CO): the black
 309 solid line represents the mean while the shaded grey error bar represent mean \pm std. The vertical dashed lines mark
 310 the beginning (left one) and the end (right one) of the PLR.
 311

312 Figure 5 shows, on the same timescale, the averaged (across subjects) time course of IVC
 313 collapsibility indexes, namely CI, RCI and aCCI (with CCI superimposed as dashed line). Here

314 the variations with respect to the mean baseline values are not translated in percentage terms,
315 since the indexes are already expressed as percentages, so that absolute variations (of a
316 percentage) are considered (i.e., DELTA in absolute terms). It can be observed that all indices
317 exhibit a consistent decrease, which is maintained throughout PLR, and that aCCI exhibited a
318 sharper decrease at the beginning of PLR, compared to CI and RCI.

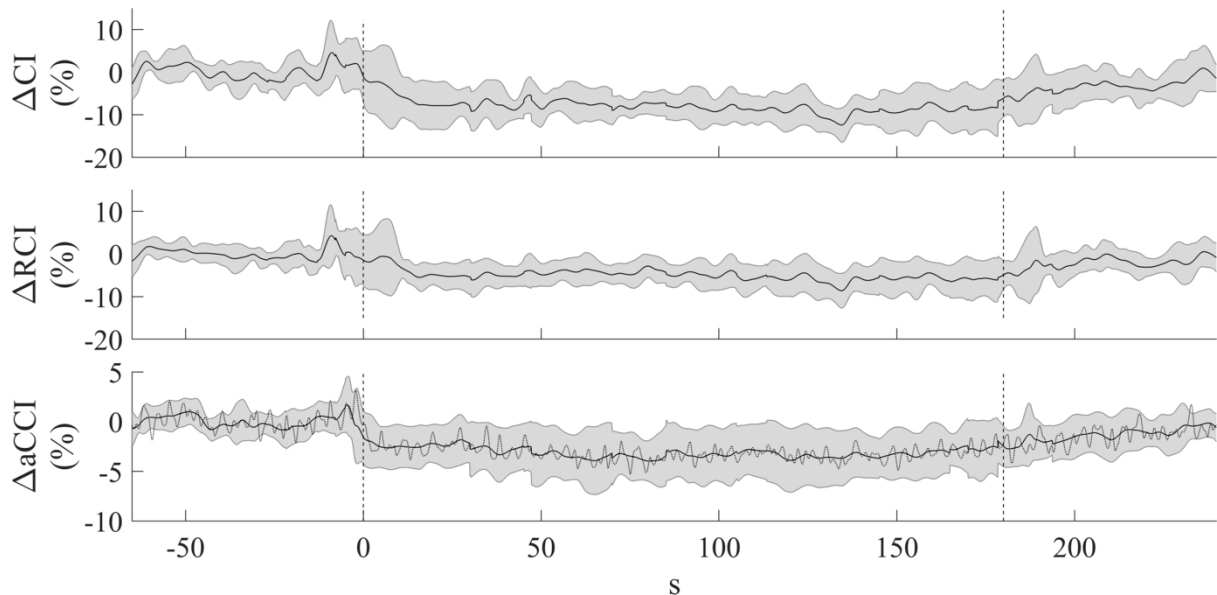
319 In Table 1, the values averaged across subjects for baseline, PLR, and DELTA (in
320 percentage terms) for all the physiological variables of interest are listed, as well as the
321 statistical significance against the null hypothesis of no effects induced by PLR. As it can be
322 noticed, HR and MAP did not change following PLR while CO and all the IVC collapsibility
323 indexes did.

324 Finally, regarding the prediction of fluid responsiveness, both CI and aCCI performed as
325 perfect classifiers (i.e., AUCROC 1) with threshold of 21% and 9%, respectively, while RCI
326 reached a poorer performance (AUCROC 0.78).

327 *Correlations among indices*

328 The individual mutual correlations in time among the IVC collapsibility indexes are
329 reported below (the original CCI is no longer considered): the biggest correlation is between
330 CI and RCI (mean value 0.81), while the smallest one is between RCI and aCCI (mean value
331 0.2) and the intermediate one is between CI and aCCI (mean value 0.49). It is worth to mention
332 that the CI-RCI distribution presents a narrower interquartile range compared to the CI-aCCI
333 distribution, highlighting the robustness of the link between the former two indexes. Finally,
334 the Pearson correlation coefficient among the averaged baseline values of CI-RCI, CI-aCCI
335 and RCI-aCCI was 0.92 (0.66, 0.98), 0.76 (0.19, 0.95) and 0.50 (-0.25, 0.87), respectively. The
336 same coefficients for the DELTA values, following the same order, were 0.74 (0.16, 0.94),
337 0.73 (0.13, 0.94), 0.2 (-0.53, 0.76).

338



339 **Fig. 5.** Inferior Vena Cava collapsibility indexes averaged (across subjects) time course. Absolute changes with
340 respect to the mean baseline value of Caval Index (Δ CI), Respiratory Caval Index (Δ RCI) and averaged Cardiac
341 Caval Index (Δ aCCI): the black solid line represents the mean while the shaded grey error bar represents mean \pm
342 \pm std. The latter graph presents also a superimposed dashed line trace that is the native Cardiac Caval Index: note
343 the oscillations due to the respiratory modulation of the cardiac induced pulsatility which are removed in the aCCI
344 trace (black solid line). The vertical dashed lines mark the beginning (left one) and the end (right one) of the PLR.
345

346 Discussion

347 The present study allowed to confirm preliminary observations and to achieve new relevant
348 results, which can be synthesized as follows:

- 349 1) Although the CI is generally considered as an index of the respiratory-induced
350 pulsatility of the IVC, it is heavily affected (or disturbed) by a pulsatility of cardiac
351 nature.
- 352 2) The magnitude of the cardiac pulsatility of IVC is still modulated by the respiratory
353 activity, which negatively impacts on the reliability of the CCI.
- 354 3) Averaging the CCI over single respiratory cycles effectively eliminates the respiratory
355 modulation and improves its stability in time.
- 356 4) The averaged cardiac collapsibility index (aCCI) responsiveness to PLR is uncorrelated
357 to the respiratory collapsibility index (RCI), suggesting that the two indices may carry
358 different information.

359 To our knowledge, this is the first study reporting a long-term monitoring and analysis of
360 IVC pulsatility, which was achieved thanks to a newly devised experimental set-up and
361 consolidated image processing algorithms^{13,14,16,24,34}. With this approach, a continuous time
362 series of the average IVC diameter, with high time resolution, could be analysed along with
363 other physiological variables: such an analysis included the identification of the oscillatory
364 components of the IVC diameter of respiratory and cardiac origin and the automated
365 calculation of the corresponding collapsibility indices RCI and CCI (Fig. 1)¹⁶.

366 *The pivotal role of heart in Inferior Vena Cava respirophasic oscillations*

367 The aforementioned framework gave us the possibility to carefully observe the interplay
368 between respiration and heartbeat in generating the IVC pulsatility. Indeed, although IVC
369 pulsatility has been already the object of hundreds of studies^{11,12} and its use in the clinical
370 settings, as predictor of fluid responsiveness^{6,7} or as surrogate measure of central venous
371 pressure³⁴, has been extensively investigated, only recently the cardiac component of the IVC
372 pulsatility has been described²². This component was probably too weak or too fast to be
373 detected and disentangled from the slower respiratory component by means of just the visual
374 assessment and the standard tools available on US machines. On the one hand, these limitations
375 delayed the recognition and the investigation of the characteristics and meaning of the cardiac
376 component, on the other hand, the unrecognized cardiac oscillation, merging with the primary
377 respiratory oscillation, decreased the “signal-to-noise ratio” and increased the variability of the
378 oscillatory pattern. We speculate that this overlooked “disturbance” on the assessment of IVC
379 diameter may at least partly explain the poor reliability and clinical applicability of the CI^{11,12}.
380 Notably, in the present study, removal of the cardiac pulsatility reduced the IVC collapsibility
381 index by about 50% (i.e., RCI is about 50% of CI) and, accordingly, the aCCI approximately
382 accounts for the other 50% (see Table 1, baseline). These results challenge the concept that the
383 classical IVC CI quantifies the “respirophasic” changes in IVC diameter.

384 As shown in the representative recordings of Figure 1, as well as in other figures previously
385 published^{15,16}, the cardiac pulsatility is modulated by respiration: the magnitude of the
386 oscillation increases at low IVC diameter, which occurs approximately at the end of the
387 inspiratory phase (maximum lung volume). This modulatory pattern fits with the idea that the
388 pulse pressure, mainly provided by the atrial contraction, results in a lower volume increase
389 (reflected by a lower IVC diameter increase) when the IVC compliance is lower, which occurs
390 at larger IVC size (Mesin et al, *submitted*). Surprisingly an opposite pattern is shown in Figure
391 4 of the study from Sonoo et al²³, i.e., wider cardiac pulsatility during expiration compared to
392 inspiration. However, their average findings (collected from 142 patients enrolled in an
393 emergency department) confirm a higher CCI during inspiration (13.8%) compared to

394 expiration (11.0%). This modulatory action is responsible for the high CoV of the CCI in time,
395 similar to the CoV of CI (Fig. 2)¹⁶ and negatively impacts on its potential clinical usefulness.
396 By simply averaging over single respiratory cycles (aCCI), this problem was effectively
397 addressed and the CoV in time considerably reduced.

398 As discussed above, cardiac pulsatility is larger when the vessel size is smaller and vessel
399 compliance is larger. As such, aCCI candidates as a possible indicator of IVC compliance and
400 of poor vascular filling. In this respect, it is interesting to observe that it was shown to correlate
401 to CI, both in time (intra-subject) and across different subjects (in basal conditions). Moreover,
402 it was significantly affected by PLR (-28%, p<0.01).

403 On the other hand, while a similar performance was reported by RCI (good correlation with
404 CI and significant decrease during PLR), aCCI and RCI were very poorly correlated: their
405 spontaneous oscillations in resting conditions are uncorrelated, their absolute values assessed
406 in resting conditions are uncorrelated, their responses to a (simulated) fluid challenge are
407 uncorrelated. These results strongly suggest that RCI and CCI are carrier of different
408 information (although both sensitive to fluid challenges). Their different time course in the
409 response to PLR (Fig. 5, aCCI exhibiting a faster and sharper response than RCI) further
410 supports this proposition.

411 *Clinical implications*

412 While further studies are necessary to understand the distinct physio-pathological meaning
413 of the two indices and their possible integration for clinical purposes, the possibility to get
414 increased and more reliable information from the same fast and non-invasive US examination
415 is intriguing. To date, only few studies have included a cardiac IVC collapsibility index in their
416 outcomes. In particular, the presence of CCI enhanced the capacity to predict the volume status
417²⁴ and right atrial pressure in patients³⁴. However, no one has yet investigated the potential of
418 CCI in predicting a fluid challenge. For this reason, although we were curious to perform such
419 an investigation, we are aware that, given our small dataset (N=9) and the limitations of the
420 photoplethysmographic finger-cuff pulse contour analysis techniques in reliably monitoring
421 CO³⁵, the extrapolated ROC analysis presented in this work are not relevant for a valid fluid
422 responsiveness study. Beyond that, we believe that the present findings, although obtained on
423 healthy volunteers, can add new useful information to the widespread use of the IVC
424 collapsibility indexes in predicting the fluid responsiveness in patients.

425 *Physiologic response to Passive Leg Raising*

426 A final comment concerns the general response to PLR in this group of healthy subjects,
427 which provides a nice description of the physiological adaptation of the body to the new
428 situation (Figs. 4 and 5): no apparent effect on MAP, only a minor (pre-) activation of HR,
429 probably an increase in alertness due to the passive leg movement, along with a small but
430 visible transient increase in CO³². In comparison, all the IVC indices detect a net variation
431 during PLR. Interestingly the exhibited changes are not transient, but last throughout the 3-min
432 duration of the test, which likely indicates that this time is too short for adjustments in blood
433 volume. Moreover, they show that the duration of the transients is shorter at the onset (< 15 s)
434 than at the termination of PLR (about 1 min).

435 *Limitations*

436 One limitation of the study is related to the way IVC videos were acquired, i.e., with the
437 probe held in place by a probe holder rather than by the hand of the echographer. While this
438 was a necessary implementation to achieve stable recordings lasting several minutes, it is not

439 without drawbacks, as involuntary spontaneous movements of the subject as well as
440 movements resulting from the PLR manoeuvre could occasionally interrupt the correct IVC
441 tracking. However, thanks to the prompt intervention of the operators, the proper probe
442 orientation was generally restored within seconds with no impact on the subsequent analysis.
443 Prospectively, with the increasing adoption of 4D US machines, the edge-tracking will be likely
444 extended to 3D images, which will minimize misalignment problems related to latero-lateral
445 displacement of IVC: at present, a potential confounding factor in long-axis imaging of IVC,
446 irrespective of whether the US probe is held by hand or fixed supports.

447 Secondly, the experiment was performed only on healthy volunteers posing some
448 limitations to the extrapolation of the results to the clinical setting. Moreover, we had to exclude
449 subjects that could not present good quality imaging of the IVC, as required by the image
450 processing routines. This criterion slightly biased the recruited sample towards a prevalence of
451 males, possibly due to their lower thickness of abdominal adipose tissue layer. However, we
452 are not aware of sex-related differences in IVC indices that could have affected the general
453 validity of the present results. Unfortunately, this is a known limitation of US studies that
454 require high quality imaging.

455 Finally, the possibility exists that CCI could be influenced by additional factors related to
456 pathological alterations of cardiac function (concerning rhythm, contractility, stiffness, and
457 valvular efficiency), of other variables such as pulmonary arterial pressure and intra-abdominal
458 pressure, as well as of hemodynamic phenomena at the confluence of superior and inferior vena
459 cava. These pathological states may alter the magnitude and the morphology of the cardiac
460 component of CVP pulsatility irrespective or in addition to the mean CVP value. For instance,
461 in atrial fibrillation the absence of the atrial systole and the irregularity of the ventricular
462 rhythm would profoundly alter the pulsatile pattern of right atrial pressure. This is likely to
463 introduce a pathology-dependent variability in the absolute value of CCI, although relative
464 changes in CCI should still effectively detect or monitor acute changes in CVP and volume
465 status. The influence of pathological conditions on the CCI remains to be explored through
466 further studies on specific patient populations.

467 *Conclusions*

468 With this methodological study on healthy subjects, we evidenced that through echographic
469 long-term monitoring of the IVC longitudinal section, in association with an automated edge
470 tracking software, it is possible to record the IVC diameter and distinct respiratory and cardiac
471 collapsibility indexes as continuous time-series. A newly defined *averaged cardiac*
472 *collapsibility index*, aCCI, exhibited 1) the lowest variability in time, 2) good sensitivity to
473 simulated blood volume changes, as induced by PLR and 3) poor correlation with the RCI in
474 time, among subjects, and in their response to PLR, supporting the hypothesis that they carry
475 different information. Therefore, we believe that aCCI has the potential to overcome the poor
476 reliability of the classical CI in the fluid responsiveness prediction. Further studies in patients
477 are needed to understand its specificity and explore its applicability in the clinical practice.
478

479 **Funding Information**

480 This activity was supported by local grants (ROAS_RILO_17_01), University of Torino,
481 and by Proof of Concept “Vein Image Processing for Edge Rendering – VIPER”, supported by
482 the Italian Ministry of Economic Development, CUP C16I20000080006.

483 **Conflict of Interest**

484 An instrument implementing the algorithm used in this report to automatically track IVC
485 edges and to extract the mean IVC diameter was patented by Politecnico of Torino and
486 University of Torino (WO 2018/134726).
487

488 **References**

- 489 1. Bentzer P, Griesdale DE, Boyd J, MacLean K, Sirounis D, Ayas NT. Will This
490 Hemodynamically Unstable Patient Respond to a Bolus of Intravenous Fluids? *JAMA*.
491 2016;316(12):1298-1309. doi:10.1001/JAMA.2016.12310
- 492 2. Sakr Y, Rubatto Birri PN, Kotfis K, et al. Higher Fluid Balance Increases the Risk of
493 Death from Sepsis: Results from a Large International Audit*. *Crit Care Med*.
494 2017;45(3):386-394. doi:10.1097/CCM.0000000000002189
- 495 3. Malbrain MLNG, Van Regenmortel N, Saugel B, et al. Principles of fluid management
496 and stewardship in septic shock: it is time to consider the four D's and the four phases
497 of fluid therapy. *Ann Intensive Care*. 2018;8(1):66. doi:10.1186/s13613-018-0402-x
- 498 4. Silva JM, de Oliveira AMR, Nogueira FAM, et al. The effect of excess fluid balance
499 on the mortality rate of surgical patients: a multicenter prospective study. *Crit Care*.
500 2013;17(6):R288. doi:10.1186/cc13151
- 501 5. Monnet X, Marik PE, Teboul J-L. Prediction of fluid responsiveness: an update. *Ann*
502 *Intensive Care*. 2016;6(1):1-11. doi:10.1186/S13613-016-0216-7
- 503 6. Monnet X, Teboul JL. Assessment of fluid responsiveness: Recent advances. *Curr*
504 *Opin Crit Care*. 2018;24(3):190-195. doi:10.1097/MCC.0000000000000501
- 505 7. Shi R, Monnet X, Teboul JL. Parameters of fluid responsiveness. *Curr Opin Crit Care*.
506 2020;26(3):319-326. doi:10.1097/MCC.0000000000000723
- 507 8. Bednarczyk JM, Fridfinnson JA, Kumar A, et al. Incorporating Dynamic Assessment
508 of Fluid Responsiveness Into Goal-Directed Therapy: A Systematic Review and Meta-
509 Analysis. *Crit Care Med*. 2017;45(9):1538-1545.
510 doi:10.1097/CCM.0000000000002554
- 511 9. Ermini L, Chiarello NE, De Benedictis C, Ferraresi C, Roatta S. Venous Pulse Wave
512 Velocity variation in response to a simulated fluid challenge in healthy subjects.
513 *Biomed Signal Process Control*. 2021;63(102177). doi:10.1016/j.bspc.2020.102177
- 514 10. Long E, Oakley E, Duke T, Babl FE. Does Respiratory Variation in Inferior Vena
515 Cava Diameter Predict Fluid Responsiveness: A Systematic Review and Meta-
516 Analysis. *Shock*. 2017;47(5):550-559. doi:10.1097/SHK.0000000000000801
- 517 11. Das SK, Choupoo NS, Pradhan D, Saikia P, Monnet X. Diagnostic accuracy of inferior
518 vena caval respiratory variation in detecting fluid unresponsiveness: a systematic
519 review and meta-analysis. *Eur J Anaesthesiol*. 2018;35(11):831-839.
520 doi:10.1097/EJA.0000000000000841
- 521 12. Orso D, Paoli I, Piani T, Cilenti FL, Cristiani L, Guglielmo N. Accuracy of
522 Ultrasonographic Measurements of Inferior Vena Cava to Determine Fluid
523 Responsiveness: A Systematic Review and Meta-Analysis. *J Intensive Care Med*.
524 2020;35(4):354-363. doi:10.1177/0885066617752308
- 525 13. Mesin L, Pasquero P, Albani S, Porta M, Roatta S. Semi-automated Tracking and
526 Continuous Monitoring of Inferior Vena Cava Diameter in Simulated and
527 Experimental Ultrasound Imaging. *Ultrasound Med Biol*. 2015;41(3):845-857.
528 doi:10.1016/J.ULTRASMEDBIO.2014.09.031
- 529 14. Mesin L, Pasquero P, Roatta S. Tracking and Monitoring Pulsatility of a Portion of
530 Inferior Vena Cava from Ultrasound Imaging in Long Axis. *Ultrasound Med Biol*.
531 2019;45(5):1338-1343. doi:10.1016/J.ULTRASMEDBIO.2018.10.024
- 532 15. Mesin L, Pasquero P, Roatta S. Multi-directional Assessment of Respiratory and
533 Cardiac Pulsatility of the Inferior Vena Cava From Ultrasound Imaging in Short Axis.
534 *Ultrasound Med Biol*. 2020;46(12):3475-3482.
535 doi:10.1016/J.ULTRASMEDBIO.2020.08.027
- 536 16. Mesin L, Giovinazzo T, D'Alessandro S, et al. Improved Repeatability of the

- 537 Estimation of Pulsatility of Inferior Vena Cava. *Ultrasound Med Biol.*
538 2019;45(10):2830-2843. doi:10.1016/J.ULTRASMEDBIO.2019.06.002
- 539 17. Tobin MJ, Mador MJ, Guenther SM, Lodato RF, Sackner MA. Variability of resting
540 respiratory drive and timing in healthy subjects. *J Appl Physiol.* 1988;65(1):309-317.
541 doi:10.1152/JAPPL.1988.65.1.309
- 542 18. Gignou L, Roger C, Bastide S, et al. Influence of Diaphragmatic Motion on Inferior
543 Vena Cava Diameter Respiratory Variations in Healthy Volunteers. *Anesthesiology.*
544 2016;124(6):1338-1346. doi:10.1097/ALN.0000000000001096
- 545 19. Folino A, Benzo M, Pasquero P, et al. Vena Cava Responsiveness to Controlled
546 Isovolumetric Respiratory Efforts. *J Ultrasound Med.* 2017;36(10):2113-2123.
547 doi:10.1002/JUM.14235
- 548 20. Kimura BJ, Dalugdugan R, Gilcrease III GW, Phan JN, Showalter BK, Wolfson T.
549 The effect of breathing manner on inferior vena caval diameter†. *Eur J Echocardiogr.*
550 2011;12(2):120-123. doi:10.1093/ejechocard/jeq157
- 551 21. Bortolotti P, Colling D, Colas V, et al. Respiratory changes of the inferior vena cava
552 diameter predict fluid responsiveness in spontaneously breathing patients with cardiac
553 arrhythmias. *Ann Intensive Care.* 2018;8(1):79. doi:10.1186/s13613-018-0427-1
- 554 22. Nakamura K, Tomida M, Ando T, et al. Cardiac variation of inferior vena cava: new
555 concept in the evaluation of intravascular blood volume. *J Med Ultrason.*
556 2013;40(3):205-209. doi:10.1007/S10396-013-0435-6
- 557 23. Sonoo T, Nakamura K, Ando T, et al. Prospective analysis of cardiac collapsibility of
558 inferior vena cava using ultrasonography. *J Crit Care.* 2015;30(5):945-948.
559 doi:10.1016/J.JCRC.2015.04.124
- 560 24. Mesin L, Roatta S, Pasquero P, Porta M. Automated volume status assessment using
561 Inferior Vena Cava pulsatility. *Electronics.* 2020;9(10):1671.
562 doi:https://doi.org/10.3390/electronics9101671
- 563 25. Hagan RD, Diaz FJ, Horvath SM. Plasma volume changes with movement to supine
564 and standing positions. *J Appl Physiol.* 1978;45(3):414-418.
565 doi:10.1152/JAPPL.1978.45.3.414
- 566 26. Finnerty NM, Panchal AR, Boulger C, et al. Inferior Vena Cava Measurement with
567 Ultrasound: What Is the Best View and Best Mode? *West J Emerg Med.*
568 2017;18(3):496. doi:10.5811/WESTJEM.2016.12.32489
- 569 27. Messere A, Ceravolo G, Franco W, Maffiolo D, Ferraresi C, Roatta S. Increased tissue
570 oxygenation explains the attenuation of hyperemia upon repetitive pneumatic
571 compression of the lower leg. *J Appl Physiol.* 2017;123(6):1451-1460.
572 doi:10.1152/jappphysiol.00511.2017
- 573 28. Messere A, Turturici M, Millo G, Roatta S. Repetitive muscle compression reduces
574 vascular mechano-sensitivity and the hyperemic response to muscle contraction. *J*
575 *Physiol Pharmacol.* 2017;68(3):427-437.
- 576 29. Messere A, Tschakovsky M, Seddone S, et al. Hyper-Oxygenation Attenuates the
577 Rapid Vasodilatory Response to Muscle Contraction and Compression. *Front Physiol.*
578 2018;9:1078. doi:10.3389/fphys.2018.01078
- 579 30. Ermini L, Ferraresi C, De Benedictis C, Roatta S. Objective Assessment of Venous
580 Pulse Wave Velocity in Healthy Humans. *Ultrasound Med Biol.* 2020;46(3):849-854.
581 doi:10.1016/j.ultrasmedbio.2019.11.003
- 582 31. Kay SM. *Modern Spectral Estimation: Theory and Application.* Pearson Education
583 India; 1988.
- 584 32. Monnet X, Teboul J-L. Passive leg raising: five rules, not a drop of fluid! *Crit Care.*
585 2015;19(1):18. doi:10.1186/s13054-014-0708-5
- 586 33. Mesquida J, Gruartmoner G, Ferrer R. Passive leg raising for assessment of volume

- 587 responsiveness: A review. *Curr Opin Crit Care*. 2017;23(3):237-243.
588 doi:10.1097/MCC.0000000000000404
- 589 34. Albani S, Pinamonti B, Giovinazzo T, et al. Accuracy of right atrial pressure
590 estimation using a multi-parameter approach derived from inferior vena cava semi-
591 automated edge-tracking echocardiography: a pilot study in patients with
592 cardiovascular disorders. *Int J Cardiovasc Imaging*. 2020;36(7):1213-1225.
593 doi:10.1007/s10554-020-01814-8
- 594 35. Saugel B, Hoppe P, Nicklas JY, et al. Continuous noninvasive pulse wave analysis
595 using finger cuff technologies for arterial blood pressure and cardiac output monitoring
596 in perioperative and intensive care medicine: a systematic review and meta-analysis.
597 *Br J Anaesth*. 2020;125(1):25-37. doi:10.1016/j.bja.2020.03.013
598